Research Square

Preprints are preliminary reports that have not undergone peer review.
They should not be considered conclusive, used to inform clinical practice,
or referenced by the media as validated information.

Volumetric Analysis of Infratentorial Cerebro Spinal Fluid Compartments in Malignant Cerebral Edema

Siddharth Srinivasan
University of Nebraska Medical Center
Bahman Kargarbahrkhazar
University of Nebraska at Omaha
Yeer Jin
Creighton University
Logan Anderson
University of Nebraska Medical Center
Anna Pipinos
Creighton University
Brett Thorell
University of Nebraska Medical Center
Aurshon Bavari
University of Nebraska at Omaha
Majid Jadidi
University of Nebraska at Omaha
Daniel Surdell
University of Nebraska Medical Center
Mithun Sattur
msattur@unmc.edu
University of Nebraska Medical Center

Research Article

Keywords: Cerebral edema, Cerebrospinal fluid, Cisterna magna, Posterior fossa, Computed tomography, Volumetric segmentation

Posted Date: November 26th, 2026

DOI: https://doi.org/10.21203/rs.3.rs-11474065/v1

License: This work is licensed under a Creative Commons Attribution 4.0 International License. Read Full License

Additional Declarations: No competing interests reported.

Abstract

Background

Cisternal effacement in severe cerebral edema is conventionally assessed qualitatively, whereas cerebrospinal fluid (CSF) volumetric studies have largely focused on supratentorial spaces or evaluated the aggregated infratentorial compartments. Residual CSF volumes within individual posterior fossa compartments remain poorly characterized in patients with malignant cerebral edema requiring supratentorial decompressive hemicraniectomy. We therefore quantified compartment-specific posterior fossa CSF volumes on preoperative computed tomography in this population.

Methods

This single-center retrospective study included 114 adults undergoing decompressive hemicraniectomy following traumatic brain injury, ischemic stroke, intracerebral hemorrhage, or aneurysmal subarachnoid hemorrhage. Five compartments were segmented on preoperative 0.625-mm computed tomography: cisterna magna, quadrigeminal cistern, supracerebellar cistern, ventrolateral peri-brainstem compartment, and fourth ventricle. Primary posterior fossa pathology and hemorrhage involving target spaces were excluded. The primary endpoint was measurable cisterna magna volume (> 0 mL). Multivariable log-linear models evaluated associations with etiology and midline shift, with false-discovery-rate correction.

Results

All five compartments were measurable in every patient (100%). Median cisterna magna volume was 9.51 mL (interquartile range, 6.26–14.08); 98.2% had ≥ 3 mL and 84.2% had ≥ 5 mL. All 13 patients with midline shift ≥ 15 mm had ≥ 3 mL. Cisterna magna volume was not significantly associated with etiology (P = 0.47) or midline shift (P = 0.18). Only ventrolateral peri-brainstem volume showed an etiologic association in primary adjusted models (q = 0.041), which did not persist in sensitivity analysis (q = 0.074).

Conclusion

In this selected surgical cohort, cisterna magna CSF was consistently measurable despite malignant supratentorial edema. Compartment-specific volumetry characterized regional variation in residual CSF volumes beyond a qualitative description of cisternal effacement.

Introduction

Malignant cerebral edema can complicate traumatic brain injury (TBI), ischemic stroke, intracerebral hemorrhage (ICH), and aneurysmal subarachnoid hemorrhage (aSAH), producing severe swelling, distortion of intracranial structures and cerebrospinal fluid (CSF) spaces.[1] On computed tomography (CT), the structural consequences of swelling are commonly described by sulcal and ventricular effacement, basal cisternal compression, and midline shift.[2, 3] Although these findings characterize mass effect, qualitative descriptions of cisternal effacement do not quantify the cerebrospinal fluid (CSF) volume remaining within individual anatomical compartments.[2, 3]

CT-based CSF volumetry offers a quantitative approach to evaluating the effects of cerebral swelling on intracranial CSF spaces.[4, 5] In hemispheric infarction, serial volumetric analysis has demonstrated reductions in CSF volume during edema progression, including changes preceding substantial midline shift. Hemispheric CSF-volume ratios and automated measurements of supratentorial and infratentorial CSF distribution have extended this approach to regional assessment.[2, 6] Microsurgical anatomical studies demonstrate that the posterior fossa and adjacent peritentorial region contain distinct cisterns organized by arachnoid membranes and their relationships to the brainstem, cerebellum, and tentorium.[7–9] These

anatomical distinctions suggest that a single descriptor of cisternal effacement may obscure differences among individual CSF spaces, providing a rationale for compartment-specific volumetric assessment. An important question not resolved by the global or hemispheric measurements is how residual CSF is distributed among individual posterior fossa compartments when supratentorial edema is severe.[2, 4–6]

In this retrospective study on patients who have undergone decompressive hemicraniectomy for malignant cerebral edema, we used thin-section preoperative CT to segment five anatomically defined CSF compartments - the cisterna magna, quadrigeminal cistern, supracerebellar cistern, ventrolateral peri-brainstem compartment, and fourth ventricle. The primary objective was to determine whether the cisterna magna (the largest CSF compartment) remained volumetrically measurable on preoperative imaging across the included etiologies. Additional analyses characterized compartment-specific volumes, examined their associations with etiology, midline shift, and edema distribution.

Methods

Study Design and Cohort

This Institutional Review Board -approved, single-center retrospective cohort included 114 adults undergoing supratentorial decompressive hemicraniectomy for malignant cerebral edema secondary to aneurysmal subarachnoid hemorrhage (aSAH), traumatic brain injury (TBI), intracerebral hemorrhage (ICH), or ischemic stroke between 2015 and July 1, 2026. The primary inclusion criterion was documented cerebral edema with intraoperative bulging of the brain beyond the craniectomy margins, as confirmed by retrospective review of operative records. Additional eligibility criteria were age ≥ 18 years and availability of preoperative CT with 0.625-mm sections. Patients were excluded if the bone flap was replaced during the index procedure or if they underwent posterior fossa decompression, had primary posterior fossa pathology or intrinsic cerebellar or brainstem abnormalities, or had intraventricular hemorrhage involving the aqueduct, fourth ventricle, or posterior fossa CSF spaces. Hemorrhage confined to the lateral or third ventricles was permitted provided that the target compartments were free of blood and suitable for segmentation. Cisternal effacement was not considered segmentation failure: compartments without identifiable CSF-attenuation voxels within prespecified boundaries were assigned 0 mL. Discernible residual CSF was segmented. The study was designed as a cross-sectional assessment of posterior fossa CSF volumes at a single preoperative time point, rather than an evaluation of ICP-directed treatment or therapeutic response. Invasive ICP monitoring was available in only 18 patients (15.8%), and analyses involving recorded ICP were restricted to descriptive subgroup assessments. Accordingly, eligibility was based on documented cerebral swelling rather than a prespecified/refractory ICP threshold. CSF diversion before the analyzed CT was, however, recorded and included as a covariate in the multivariable models. The methodology proposed in the included STROBE checklist was followed.

Imaging Definitions and Segmentation

Anonymized DICOM data were imported into Mimics Research 26.0 (Materialise NV, Leuven, Belgium) and reviewed in orthogonal planes with CSF-optimized windowing. Five compartments were defined a priori, as follows.

Cisterna Magna

The cisterna magna comprised the posterior cerebellomedullary space dorsal to the lower medulla/cervicomedullary junction, inferior to the vermis and tonsils, and anterior to the occipital table. The McRae plane was the inferior limit. CSF below the foramen magnum was excluded. Lateral boundaries were parasagittal planes through the tonsillar margins. CSF contiguous with the lateral medulla was assigned to the perimedullary compartment. Roof-enclosed CSF at the fourth-ventricular outlet was ventricular. Open retromedullary CSF was cisterna magna. Folial sulci, tonsillobiventral fissures, and narrow cerebellar fissures were excluded.

Fourth Ventricle, Quadrigeminal Cistern, Supracerebellar Cistern and Ventrolateral peribrainstem cistern

The fourth ventricle extended from the caudal aqueduct to the obex, including lateral recesses to the foramina of Luschka and excluding the aqueduct, central canal, and CSF beyond the apertures. The quadrigeminal cistern was dorsal to the tectum, inferior to the splenium/posterior thalami, superior to the superior medullary velum, lingula, and rostral superior vermis, and bounded laterally by the tectal margins. Lateral midbrain CSF was perimesencephalic. Its posterior boundary was a coronal plane through the tentorial apex/falcotentorial junction at the anterior straight sinus, a CT-visible surrogate for the cerebellar precentral membrane. Posterior CSF constituted the supracerebellar compartment, including CSF over the rostral vermis and superior cerebellar surfaces. The ventrolateral peri-brainstem compartment included ventral/lateral perimesencephalic, peripontine, and perimedullary spaces from the interpeduncular, crural, and ambient cisterns to the McRae plane, including cerebellomesencephalic, cerebellopontine, and cerebellomedullary cisterns. (Figs. 1–2)

CSF was isolated using an initial − 50 to + 25 HU threshold, adjusted per patient, followed by region growing, exclusion of nonconnected background, split-mask separation, slice-by-slice manual correction, 3D reconstruction, anatomical partitioning, and volume extraction. Two operators independently repeated all five segmentations in 10 CT examinations. Absolute agreement was assessed using two-way mixed-effects, single-measure intraclass correlation coefficients with 95% CIs.

Variables and Outcomes

Recorded variables were age, sex, etiology, midline shift, IVH, hydrocephalus, insult-to-scan interval, pre-scan CSF diversion, including external ventricular drainage, and invasive intracranial pressure (ICP) monitoring. When present, intra-axial hematoma volume was estimated using ABC/2. Maximum pre-decompression ICP was categorized as < 10, 10–15, 16–20, or > 20 mm Hg.

Statistical analysis

Continuous and categorical data are reported as median (IQR) and n (%), respectively. The primary endpoint was measurable cisterna magna volume (> 0 mL). Proportions used exact Clopper-Pearson 95% CIs. Compartment volumes were compared across etiologies using Kruskal-Wallis tests (ε^2), Benjamini-Hochberg FDR correction across five omnibus tests, and Dwass-Steel-Critchlow-Fligner post hoc comparisons when significant. Log-transformed volumes were modeled using HC3-robust multivariable linear regression adjusted for etiology, age per 10 years, sex, midline shift per 5 mm, and pre-CT CSF diversion (aSAH reference). Sensitivity models additionally included IVH and hydrocephalus. Injury-to-scan and scan-to-surgery intervals were descriptive only. Exponentiated coefficients are adjusted geometric mean ratios (aGMRs; <1 indicates lower volume). Overall etiology was evaluated using 3-df robust Wald F tests. FDR correction was applied separately across five etiology and five midline-shift tests. Etiologic contrasts used nominal 95% CIs for estimation only. Among patients with ICP data, four prespecified ICP categories were assessed using exact permutation Kruskal-Wallis and exact Spearman tests. Exploratory aggregate volumes used unadjusted Kruskal-Wallis tests (ε^2). Minimum volumes, high-severity subgroup findings, and ≥ 1-, ≥ 3-, and ≥ 5-mL thresholds were descriptive. Tests were two-sided. nominal $P<.05$ was reported, whereas adjusted significance required FDR $q<.05$ or Holm-adjusted $P<.05$, as applicable. Analyses used Jamovi 2.7.22 (GAMLj 3.6.5) and R 4.5.2 in RStudio on macOS.

Results

Cohort Characteristics

The cohort comprised 114 adults: 48 with traumatic brain injury (TBI), 40 with ischemic stroke, 17 with intracerebral hemorrhage (ICH), and 9 with aneurysmal subarachnoid hemorrhage (aSAH). Median age was 49.0 years (IQR, 36.2–60.8),

57.0% were male, and median midline shift was 7.0 mm (IQR, 4.0–10.0) (Table 1).

Table 1
Cohort characteristics

Characteristic	Overall	ICH	Ischemic stroke	SAH	TBI
N	114	17	40	9	48
Age, y	49.0 (36.2–60.8)	49.0 (37.0–67.0)	53.0 (39.8–61.0)	43.0 (38.0–46.0)	43.5 (33.5–58.5)
Male sex	65 (57.0%)	8 (47.1%)	21 (52.5%)	2 (22.2%)	34 (70.8%)
Midline shift, mm	7.0 (4.0–10.0)	9.0 (7.0–10.0)	6.5 (4.0-8.7)	3.0 (0.0–7.0)	8.3 (5.0–12.0)
IVH	23 (20.2%)	9 (52.9%)	1 (2.5%)	6 (66.7%)	7 (14.6%)
Hydrocephalus	21 (18.4%)	4 (23.5%)	5 (12.5%)	5 (55.6%)	7 (14.6%)
CSF diversion before index CT	15 (13.2%)	0 (0.0%)	1 (2.5%)	6 (66.7%)	8 (16.7%)
ICP monitoring	18 (15.8%)	1 (5.9%)	2 (5.0%)	4 (44.4%)	11 (22.9%)
Insult-to-scan interval, h	16.51 (1.83–42.47)	7.42 (2.88–14.75)	37.69 (29.00-56.49)	39.33 (10.82–66.73)	2.16 (1.08–13.20)
Scan-to-surgery interval, h	3.00 (1.72–6.21)	1.78 (1.48–3.55)	5.54 (3.25–10.56)	8.82 (4.77–9.93)	2.28 (1.32–3.10)

Note: Values are median (interquartile range) or n (%). ICH: Intracerebral hemorrhage, SAH: Subarachnoid Hemorrhage, TBI: traumatic brain injury

Cisterna Magna Measurability and Volume

The cisterna magna was measurable on preoperative CT in all 114 patients (100.0%; exact 95% CI, 96.8%-100.0%), with a median volume of 9.51 mL (IQR, 6.26–14.08; range, 1.16–23.75). All patients had ≥ 1 mL, 112 (98.2%) had ≥ 3 mL, and 96 (84.2%) had ≥ 5 mL. These post hoc volume thresholds were descriptive and were not validated procedural criteria. Unadjusted cisterna magna volume did not differ across etiologies (P=.14), and no pairwise comparison was significant (Table 2).

Table 2
Posterior fossa cerebrospinal fluid compartment volumes by etiology

CSF compartment	Overall	ICH	Ischemic stroke	SAH	TBI	*H*	*P*	FDR *q*	ε^2	Significant pairwise comparisons
Cisterna magna	9.51 (6.26–14.08)	11.29 (7.36–15.74)	9.65 (7.05–15.24)	5.51 (3.83–10.66)	9.31 (6.47–12.12)	5.47	.14	.18	0.05	None
Quadrigeminal cistern	1.61 (0.82–2.37)	2.11 (1.20–2.67)	1.88 (1.16–2.46)	0.69 (0.38–1.35)	1.31 (0.63–1.97)	12.85	**.005**	**.01**	0.11	ICH > SAH (P=**.04**)
Supracerebellar cistern	6.27 (3.66–9.49)	6.35 (4.17–9.60)	7.84 (5.74–10.05)	2.68 (1.61–5.08)	5.39 (3.43–8.67)	11.09	**.01**	**.012**	0.09	Ischemic stroke > SAH (P=**.01**)
Ventrolateral peribrainstem cisterns	10.84 (7.31–13.97)	13.34 (10.08–15.49)	11.98 (7.58–15.80)	5.03 (3.89–5.97)	10.21 (6.83–13.16)	18.94	**< .001**	**.001**	0.17	ICH > SAH (P=**.001**) Ischemic stroke > SAH (P=**.002**) TBI > SAH (P=**.012**)
Fourth ventricle	3.49 (2.25–5.14)	4.41 (2.20–6.94)	3.76 (2.56–5.05)	2.33 (1.54–2.71)	3.51 (2.17–5.28)	4.88	.18	.18	0.04	None

Note: Values are median (IQR). Kruskal-Wallis omnibus tests used Benjamini-Hochberg FDR correction; significant pairwise comparisons used the Dwass-Steel-Critchlow-Fligner procedure. ε^2, Kruskal-Wallis effect size; CSF, cerebrospinal fluid; FDR, false discovery rate; ICH, intracerebral hemorrhage; IQR, interquartile range; SAH, subarachnoid hemorrhage; TBI, traumatic brain injury.

Compartment-Specific Posterior Fossa CSF Volumes

Quadrigeminal (P=.005; FDR q=.01; ε^2=.11), supracerebellar (P=.01; q=.012; ε^2=.09), and ventrolateral peri-brainstem volumes (P<.001; q=.001; ε^2=.17) differed across etiologies, driven by lower volumes in aSAH. Significant pairwise comparisons are detailed in Table 2. Fourth-ventricular volume did not differ (P=.18; q=.18). All five compartments had nonzero measurable volume in every patient. However, minimum non-cisterna magna volumes ranged from 0.005 to 0.116 mL (Supplementary Table S1).

Multivariable Analyses

After adjustment, etiology remained associated only with ventrolateral peri-brainstem volume after FDR correction (omnibus P=.008; q=.041). Relative to aSAH, aGMRs were 3.01 (95% CI, 1.35–6.74) for ICH, 2.57 (95% CI, 1.15–5.71) for ischemic stroke, and 2.15 (95% CI, 0.96–4.82) for TBI. Cisterna magna volume was associated with neither etiology (P=.47; q=.49) nor midline shift (aGMR per 5 mm, 0.93; 95% CI, 0.83–1.04; P=.18; q=.30). No other association remained significant after FDR correction. (Table 3) Additional adjustment for IVH and hydrocephalus did not materially alter the cisterna magna findings. However, the association between etiology and ventrolateral peri-brainstem volume no longer met the FDR threshold for significance (P = .015; q = .074). (Supplementary Table S2).

Table 3
Multivariable associations of etiology and midline shift with CSF compartment volumes, using SAH as the reference category

Outcome	ICH vs SAH aGMR (95% CI)	Ischemic stroke vs SAH aGMR (95% CI)	TBI vs SAH aGMR (95% CI)	Omnibus etiology F (3,106); P; FDR q	Per 5-mm shift aGMR (95% CI); P; FDR q
Cisterna magna	1.612 (0.86–3.01)	1.508 (0.83–2.74)	1.403 (0.78–2.52)	0.86; .47; .49	0.928 (0.83–1.04); .18; .30
Quadrigeminal cistern	2.492 (0.83–7.45)	1.991 (0.70–5.64)	1.516 (0.51–4.53)	2.47; .07; .11	0.924 (0.76–1.13); .43; .43
Supracerebellar cistern	2.897 (1.37–6.14)	2.612 (1.31–5.21)	2.090 (1.06–4.13)	3.00; .03; .08	0.821 (0.70–0.97); .02; .10
Ventrolateral peri-brainstem compartment	3.012 (1.35–6.74)	2.565 (1.15–5.71)	2.153 (0.96–4.82)	4.12; **.008; .04**	0.920 (0.79–1.07); .28; .35
Fourth ventricle	1.482 (0.50–4.37)	1.783 (0.80–3.99)	1.667 (0.73–3.83)	0.81; .49; .49	0.819 (0.61–1.09); .17; .30

Each model used the natural logarithm-transformed compartment volume as the dependent variable and included etiology, age per 10 years, sex, midline shift per 5 mm, and cerebrospinal fluid diversion before the analyzed computed tomography scan. Models were fitted in all 114 patients using HC3 heteroscedasticity-robust standard errors and t-based 95% confidence intervals. Adjusted geometric mean ratios (aGMRs) greater than 1.00 indicate greater model-estimated geometric mean volume relative to subarachnoid hemorrhage. For midline shift, aGMRs below 1.00 indicate lower volume for each additional 5 mm of shift. Overall etiology P values were obtained using 3-degree-of-freedom robust Wald F tests. False-discovery-rate (FDR) correction was applied separately across the five compartment-specific overall etiology tests and the five midline-shift tests. Individual etiologic 95% CIs are nominal and are presented for estimation. Bold indicates FDR q<.05. CI indicates confidence interval CSF, cerebrospinal fluid; CT, computed tomography; ICH, intracerebral hemorrhage; SAH, subarachnoid hemorrhage; and TBI, traumatic brain injury.

High-Severity Subgroups and ICP

The cisterna magna remained measurable in every prespecified high-severity subgroup. Among patients with midline shift ≥ 10 mm (n = 32), median volume was 8.05 mL. 31 (96.9%) had ≥ 3 mL and 25 (78.1%) had ≥ 5 mL. Among those with midline shift ≥ 15 mm (n = 13), median volume was 6.04 mL. All had ≥ 3 mL and 10 (76.9%) had ≥ 5 mL. It was also measurable in all patients with hydrocephalus, IVH, or prior CSF diversion (Supplementary Table S3). Compartment volumes did not differ according to intraparenchymal hematoma volume (< 40 vs ≥ 40 cm^3; all P≥.51).

Among 18 patients with ICP data, the cisterna magna was measurable in all. Fourteen had ICP > 20 mm Hg. Their median cisterna magna volume was 8.74 mL, and 11 had ≥ 5 mL. Volume did not differ across ICP categories (P=.42), nor was the correlation significant (Spearman ρ = .42; exact P=.08). These analyses were descriptive.

Edema Distribution and Interrater Reproducibility

Unilateral and bilateral/diffuse edema each occurred in 57 patients. Unilateral edema was associated with greater ventrolateral peri-brainstem volume (aVR, 1.28; 95% CI, 1.07–1.53; Holm-adjusted P=.040), whereas cisterna magna volume did not differ (aVR, 1.12; 95% CI, 0.93–1.36; P=.21). No other compartment remained significant after correction (Supplementary Table S4).

Interrater ICCs (95% CIs) were 0.89 (0.63–0.97) for the cisterna magna, 0.88 (0.54–0.97) for the quadrigeminal cistern, 0.94 (0.77–0.99) for the supracerebellar cistern, 0.89 (0.61–0.97) for the ventrolateral peri-brainstem compartment, and 0.77 (0.34–0.94) for the fourth ventricle.

Discussion

In this cohort of 114 adults undergoing decompressive hemicraniectomy for malignant cerebral edema, the cisterna magna remained radiographically measurable despite severe supratentorial swelling (median, 9.51 mL); 98.2% retained ≥ 3 mL and

84.2% retained ≥ 5 mL. It remained measurable in all 13 patients with midline shift ≥ 15 mm, all 14 with recorded ICP > 20 mm Hg, and all 15 who underwent supratentorial CSF diversion before the analyzed CT. Cisterna magna volume was not independently associated with etiology or increasing midline shift. In contrast, the rostral and ventrolateral compartments showed greater attenuation, particularly in aSAH, with the ventrolateral peri-brainstem compartment demonstrating the only significant adjusted etiologic association. Bilateral/diffuse edema was likewise associated with lower ventrolateral peri-brainstem volume, whereas cisterna magna volume did not differ by edema laterality.

These findings add anatomical detail to the conventional assessment of cisternal effacement in malignant cerebral edema states. Established CT classifications describe basal cisterns categorically alongside other manifestations of mass effect, including midline shift and space-occupying lesions, without separately quantifying each cisternal compartment.[3] Subsequent automated approaches have demonstrated that basal cisternal volume can be measured quantitatively together with lesion volume and midline shift, supporting a transition from categorical descriptions toward continuous structural measurements.[10] In the present study, the observation that every compartment remained technically measurable despite substantial differences in residual volume illustrates the limited discrimination of a binary present-or-absent endpoint. Compartment-specific volumetry provides additional information about the amount and location of residual CSF without requiring that a narrow or distorted space be classified as completely obliterated.

Previous investigations have primarily used CSF volumetry to characterize the evolution and severity of supratentorial swelling. Serial CT studies after hemispheric infarction demonstrated that CSF-volume reduction accompanies edema progression and may precede substantial midline shift. [4, 5] Hemispheric CSF-volume ratios subsequently provided a regional measure of asymmetric CSF displacement after ischemic stroke. [6] In TBI, automated segmentation has also been used to examine CSF distribution among the right supratentorial, left supratentorial, and infratentorial compartments.[2] They demonstrated that in patients with supratentorial mass effect requiring surgery, the supratentorial CSF volume was lower and this can potentially help in predicting the need for surgery. However, they have not individually segmented each of the infratentorial CSF compartments. The present analysis addresses a complementary question: how residual CSF is distributed among individually defined posterior fossa and adjacent infratentorial compartments on the preoperative examination at a point where the cerebral edema or supratentorial mass effect was severe enough to warrant a decompressive hemicraniectomy. Unlike longitudinal measurements of CSF depletion, these measurements describe the anatomical configuration present at a selected point in the course of malignant cerebral edema.

Anatomical subdivision is relevant because these spaces differ in their boundaries and relationships to the surrounding neural structures.[9] Microsurgical studies describe the posterior fossa and peritentorial cisterns as distinct spaces organized by arachnoid membranes and their relationships to the brainstem, cerebellum, and tentorium.[7–9] In our segmentation framework, the retromedullary cisterna magna was distinguished from the fourth ventricle, ventrolateral peri-brainstem spaces, and more rostral quadrigeminal and supracerebellar compartments. This separation allowed regional differences to be characterized without combining them into a single infratentorial CSF measurement. The three-dimensional reconstructions illustrate the differing shapes and spatial extents of these study-defined compartments (Figs. 1 and 2). However, their anatomical arrangement provides a framework for interpreting the observed distribution, not evidence that any compartment is mechanically protected from compression.

The etiologic comparisons further support a compartment-specific interpretation. Quadrigeminal, supracerebellar, and ventrolateral peri-brainstem volumes differed across etiologies in unadjusted analyses, with lower volumes in the aneurysmal subarachnoid hemorrhage (aSAH) group. After adjustment only the association between etiology and ventrolateral peri-brainstem volume remained significant. Neither cisterna magna nor fourth-ventricular volume showed a significant adjusted etiologic association (Tables 2 and 3). Thus, the principal between-etiology finding was localized rather than shared uniformly across the segmented spaces. Nevertheless, the aSAH subgroup was small and frequently had hydrocephalus or pre-CT CSF diversion, limiting separation of disease-related differences from treatment effects and other aspects of case mix. The observed associations should therefore be regarded as regional volumetric findings rather than evidence of a specific mechanism of cisternal compression.

The relationship with midline shift also requires a distinction between supratentorial displacement and regional CSF volume. Cisterna magna volume was not significantly associated with increasing midline shift after adjustment, with an adjusted geometric mean ratio of 0.93 per 5-mm increment in shift (95% CI, 0.83–1.04). Among the 13 patients with midline shift of at least 15 mm, the median cisterna magna volume was 6.04 mL, and all had at least 3 mL. These findings demonstrate that marked supratentorial displacement can coexist with measurable cisterna magna CSF. They do not establish that cisterna magna volume is unaffected by swelling. The distinction is consistent with previous volumetric work showing that CSF displacement and midline shift capture related but nonidentical aspects of edema evolution.[5, 6] In the present cohort, neither the magnitude of midline shift nor the persistence of an individual cistern should be interpreted as a complete description of the regional anatomical consequences of edema. Edema distribution provided a further example of regional differences. Unilateral/unihemispheric edema was associated with greater ventrolateral peri-brainstem volume than bilateral or diffuse edema, whereas no significant difference was identified for cisterna magna volume. The ventrolateral association remained significant after multiplicity correction, with an adjusted volume ratio of 1.28 (95% CI, 1.07–1.53; Holm-adjusted P=.040). Considered alongside the etiologic analysis, this finding suggests that the ventrolateral peri-brainstem compartment may capture anatomical variation not apparent from cisterna magna measurements alone. It also argues against using a single posterior fossa compartment as a surrogate for the distribution of CSF throughout the region. Whether these patterns have diagnostic or prognostic significance remains to be established (Supplementary Table S4).

The immediate contribution of this study is descriptive and anatomical. It characterizes the residual volumes of separately defined CSF spaces in patients with malignant supratentorial edema, with consistent measurability of the cisterna magna across the included etiologies. Further work should establish reference distributions using the same segmentation boundaries, evaluate within-patient changes on serial imaging, factor treatment undertaken to control cerebral edema and determine whether compartment-specific measurements add information beyond conventional CT findings. Such studies would clarify whether the observed regional patterns reflect baseline anatomical variation, differential changes during edema progression, or a combination of both while also considering the systemic pathophysiological process underlying the cerebral edema progression.

Limitations

This study has several limitations. Its retrospective, single-center design and restriction to patients undergoing decompressive hemicraniectomy limit generalizability to the broader spectrum of cerebral edema. Patients with primary posterior fossa pathology, intrinsic cerebellar or brainstem abnormalities, or hemorrhage involving the specified posterior fossa CSF spaces were excluded. Accordingly, the finding of universal cisterna magna measurability applies to the selected population with supratentorial disease and assessable target spaces, not to all causes or stages of malignant cerebral edema. Although complete effacement was not an exclusion criterion and compartments without identifiable CSF-attenuation voxels were eligible to receive a volume of 0 mL, the exclusion of blood-containing target spaces remains an important restriction on applicability. The absence of a nonedematous comparison group or preinjury imaging prevents estimation of the proportion of baseline cisternal volume remaining in individual patients. A measurable volume therefore should not be equated with normal volume or absence of compression. Measurements were also not normalized to intracranial or posterior fossa size, leaving potential contributions from interindividual anatomical variation despite adjustment for age and sex. Furthermore, analysis of a single preoperative CT obtained at variable intervals after injury cannot establish longitudinal persistence or determine the sequence of changes among compartments. Nonstandardized treatment before imaging and incomplete capture of relevant clinical variables introduce additional potential confounding. Measurement uncertainty is another consideration. Threshold-based CSF segmentation requires anatomical review and correction because attenuation overlap, noise, and artifacts can lead to tissue misclassification.[2, 11–13] Patient-specific threshold adjustment and manual boundary correction may be particularly consequential when residual spaces are small. In addition, the ventrolateral peri-brainstem mask combined several contiguous cisternal spaces, and some boundaries were defined using CT-visible anatomical surrogates rather than direct visualization of arachnoid membranes. The resulting measurements should therefore be interpreted according to the stated compartment definitions rather than assumed to be

interchangeable with differently defined cisternal volumes. Interrater assessment involved only 10 examinations, with wide confidence intervals, particularly for the fourth ventricle. Agreement in extracted volume does not by itself establish voxel-level segmentation accuracy or reproducibility across institutions, scanners, and operators. Refractory ICP, tiered medical management of cerebral edema, sedation/ventilator, and anti-osmolar treatment measures were not factored. Finally, the etiologic groups were unequal, particularly the aneurysmal subarachnoid hemorrhage subgroup of nine patients, limiting subgroup precision. The 3- and 5-mL thresholds were post hoc descriptive summaries rather than validated imaging cutoffs. The analysis also did not establish relationships with neurological outcomes or demonstrate incremental diagnostic performance over conventional CT assessment. These findings support anatomical characterization, but not the use of an isolated cisternal volume to grade edema severity or guide clinical decisions.

Conclusion

In this selected cohort of 114 adults undergoing decompressive hemicraniectomy for malignant supratentorial edema, cisterna magna cerebrospinal fluid was measurable in every patient, with a median volume of 9.51 mL. Volumes of at least 3 mL and 5 mL were identified in 98.2% and 84.2% of patients, respectively, and measurable cisterna magna CSF was also present in all patients with midline shift ≥ 15 mm. Compartment-specific volumetry characterized the amount and distribution of residual CSF within separately defined infratentorial spaces, supporting quantitative anatomical assessment beyond a binary description of cisternal effacement.

Declarations

Funding: Nebraska Research Initiative and National Institute of General Medical Sciences, (P20GM152301)

Conflict of Interest: None

Human ethics approval: This retrospective study was approved by the University of Nebraska Medical Center Institutional Ethics Committee (0409-26-EP) The study was conducted in accordance with the Declaration of Helsinki and its subsequent amendments.

Patient consent to participate: Waived off by institutional review committee for this deidentified retrospective study

Data availability statement: Data that support the findings in this study are available from the corresponding author upon reasonable request

Generative AI use: None

Acknowledgements: This study was not presented before.

Competing Interests: None

Disclosures: None

Data Availability Statement: Data that support the findings in this study are available from the corresponding author upon reasonable request

Ethics Statements:

Patient consent for publication: Waived off by the Institutional Review Board for this retrospective study presenting deidentified data.

Institutional Ethic Committee approval: Obtained

References

1. Cook AM, Morgan Jones G, Hawryluk GWJ, et al. Guidelines for the Acute Treatment of Cerebral Edema in Neurocritical Care Patients. Neurocrit Care. 2020;32:647–66. https://doi.org/10.1007/s12028-020-00959-7.
2. Puzio T, Matera K, Wiśniewski K, et al. Automated volumetric evaluation of intracranial compartments and cerebrospinal fluid distribution on emergency trauma head CT scans to quantify mass effect. Front NeuroSci. 2024;18:1341734. https://doi.org/10.3389/fnins.2024.1341734.
3. Marshall LF, Marshall SB, Klauber MR, et al. A new classification of head injury based on computerized tomography. J Neurosurg. 1991;75:S14–20. https://doi.org/10.3171/sup.1991.75.1s.0s14.
4. Dhar R, Chen Y, Hamzehloo A, et al. Reduction in Cerebrospinal Fluid Volume as an Early Quantitative Biomarker of Cerebral Edema After Ischemic Stroke. Stroke. 2020;51:462–7. https://doi.org/10.1161/STROKEAHA.119.027895.
5. Dhar R, Yuan K, Kulik T, et al. CSF Volumetric Analysis for Quantification of Cerebral Edema After Hemispheric Infarction. Neurocrit Care. 2016;24:420–7. https://doi.org/10.1007/s12028-015-0204-z.
6. Dhar R, Hamzehloo A, Kumar A, et al. Hemispheric CSF volume ratio quantifies progression and severity of cerebral edema after acute hemispheric stroke. J Cereb Blood Flow Metabolism. 2021;41:2907–15. https://doi.org/10.1177/0271678X211018210.
7. Matsuno H, Rhoton AL Jr, Peace D. Microsurgical anatomy of the posterior fossa cisterns. Neurosurgery. 1988;23:58–80. https://doi.org/10.1227/00006123-198807000-00012.
8. Vinas FC, Dujovny M, Fandino R, Chavez V. Microsurgical anatomy of the arachnoidal trabecular membranes and cisterns at the level of the tentorium. Neurol Res. 1996;18:305–12. https://doi.org/10.1080/01616412.1996.11740426.
9. Morris JA, Gilbert BC, Parker WT, Forseen SE. Anatomy of the Ventricles, Subarachnoid Spaces, and Meninges. Neuroimaging Clin N Am. 2022;32:577–601. https://doi.org/10.1016/j.nic.2022.04.005.
10. Jain S, Vande Vyvere T, Terzopoulos V, et al. Automatic Quantification of Computed Tomography Features in Acute Traumatic Brain Injury. J Neurotrauma. 2019;36:1794–803. https://doi.org/10.1089/neu.2018.6183.
11. Chen Y, Dhar R, Heitsch L, et al. Automated quantification of cerebral edema following hemispheric infarction: Application of a machine-learning algorithm to evaluate CSF shifts on serial head CTs. NeuroImage: Clin. 2016;12:673–80. https://doi.org/10.1016/j.nicl.2016.09.018.
12. Suresh VA, Srinivasan S, Opperman PJ et al. (2026) Slit ventricles in idiopathic intracranial hypertension appear to expand after venous sinus stenting: a volumetric analysis. J Neurointerv Surg jnis-2026-025625. https://doi.org/10.1136/jnis-2026-025625
13. Srinivasan S, Rasmussen J, Benck L, et al. Venous sinus stent placement is associated with improvement in volumetric skull base thickness. J NeuroInterventional Surg. 2026. https://doi.org/10.1136/jnis-2026-025367.

Figures

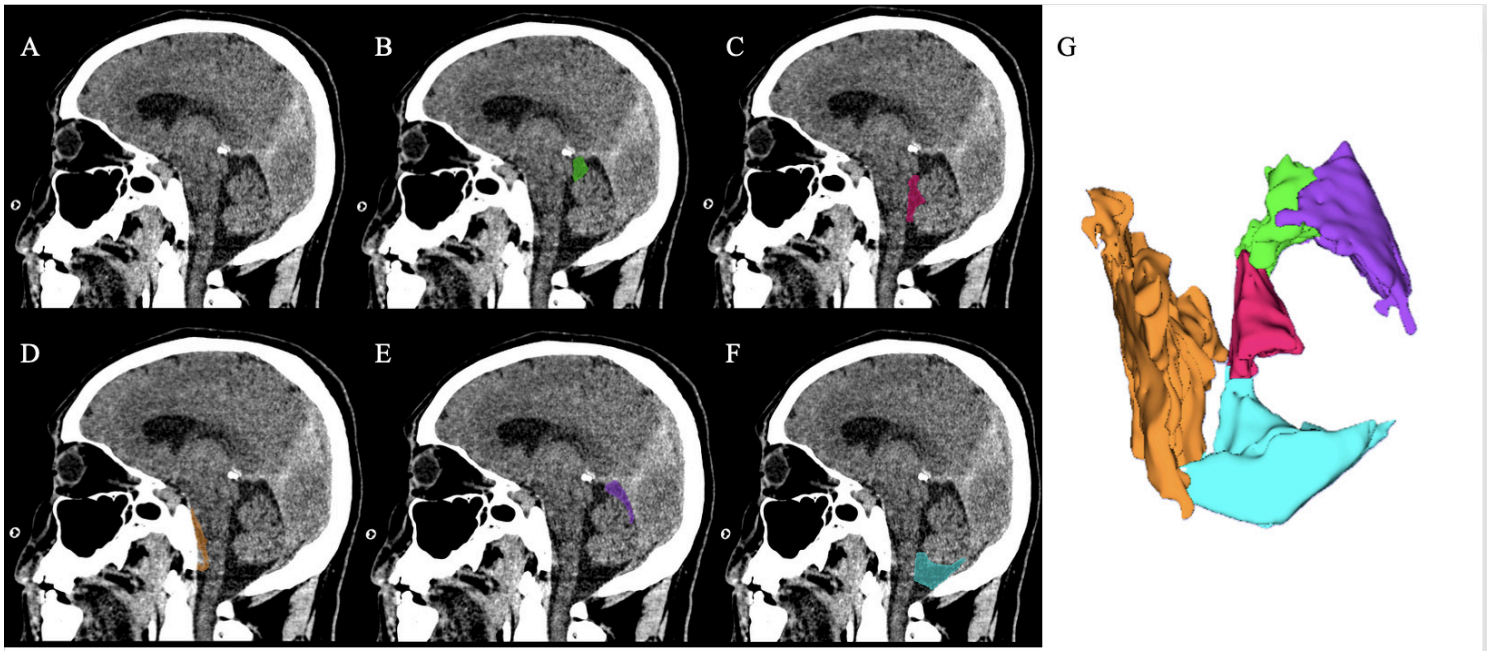

Figure 1

Posterior fossa cerebrospinal fluid compartment segmentation in a patient with a right middle cerebral artery territory infarction. (A) Preoperative midsagittal noncontrast computed tomography image obtained before decompressive hemicraniectomy, demonstrating severe supratentorial edema with marked sulcal effacement. Study-defined segmentations demonstrate the (B) quadrigeminal cistern in green, (C) fourth ventricle in maroon, (D) ventrolateral peribrainstem cistern in yellow ochre, (E) supracerebellar cistern in purple, and (F) cisterna magna in blue. (G) Three-dimensional volumetric reconstruction of all segmented compartments.

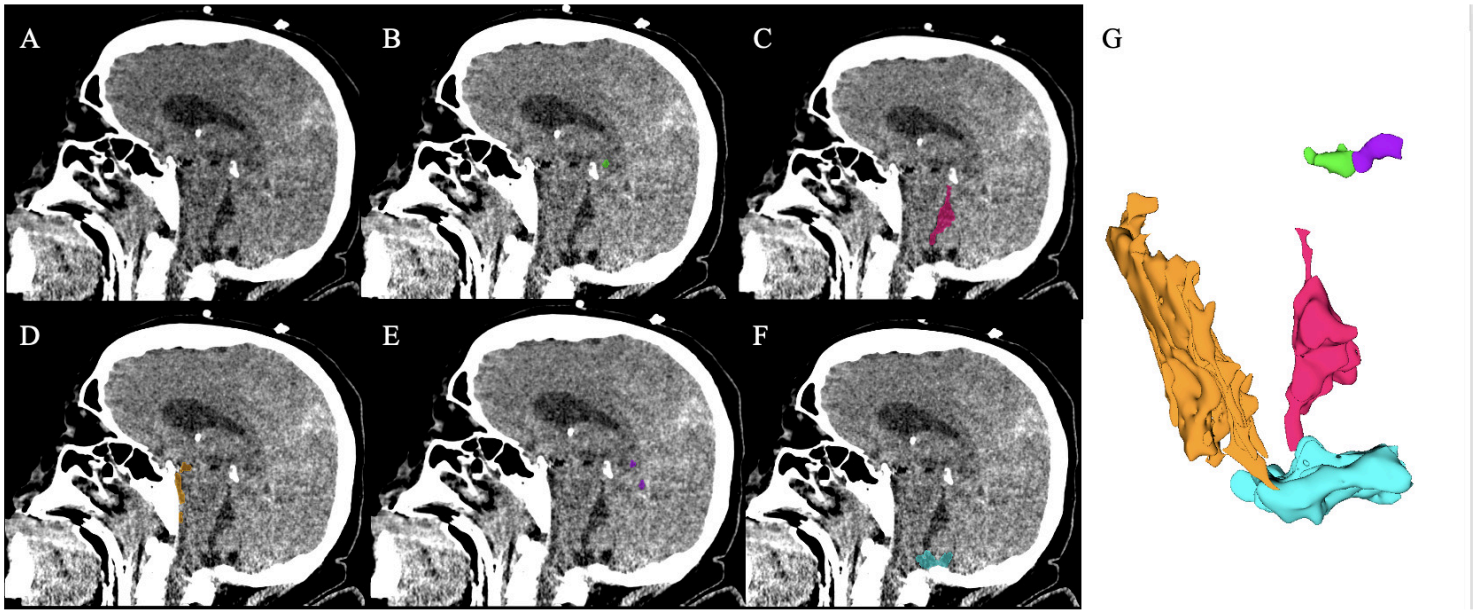

Figure 2

Posterior fossa cerebrospinal fluid compartment segmentation in a patient with aneurysmal subarachnoid hemorrhage and diffuse cerebral edema who subsequently underwent decompressive hemicraniectomy. (A) Preoperative midsagittal noncontrast computed tomography image demonstrating severe supratentorial edema. Study-defined segmentations demonstrate the (B) quadrigeminal cistern in green, (C) fourth ventricle in maroon, (D) ventrolateral peribrainstem cistern in

yellow ochre, (E) supracerebellar cistern in purple, and (F) cisterna magna in blue. The ventrolateral peribrainstem, quadrigeminal and supracerebellar cisterns depict small/near-effaced CSF space, whereas the cisterna magna is smaller but remains preserved. (G) Three-dimensional volumetric reconstruction of all segmented compartments.

Supplementary Files

This is a list of supplementary files associated with this preprint. Click to download.

- Supplementarytables.docx